JOURNAL OF MATERIALS SCIENCE 29 (1994) 3358–3362

A comparison of methods for estimating the weld-metal cooling rate in laser welds

I. GILATH
SOREQ, Yavne 70600, Israel
J. M. SIGNAMARCHEIX, P. BENSUSSAN
D.G.A., Arcveil, 94114, France

Microstructural transformations in 304 L stainless-steel welds as a function of welding parameters were studied using a high-power continuous CO_2 laser. The experimental results can be represented by the relation $\lambda_1 = 40\ V^{-1/2}$ where λ_1 is the primary dendrite spacing in μm and V is the welding speed in mm s^{-1}, for different laser powers and two sample thicknesses. The cooling rates estimated by different methods have been found to be in the range 10^2 to 3×10^3 K s^{-1}, and the temperature gradients are in the range 10^2 to 9×10^2 K cm^{-1}. The experimental results are shown to be in very good agreement with recent dendrite-growth models. An analogy is presented between the cooling rate during melt spinning and laser welding.

1. Introduction

High cooling rates are produced by the high-power-density lasers used in welding or in surface treatment. The cooling-rate range between slow (directional solidification) and high (laser- or electron-beam treatment) can be as large as nine orders of magnitude [1] or more. High temperature gradients must be recorded in very short time intervals in order to measure the cooling rate during rapid solidification of the molten pool. There are no instrumental facilities available to perform these measurements in the laser-melted zone. Therefore, indirect estimates are usually made using correlations [1–4] between the cooling rate and microstructural features such as primary- or secondary-dendrite-arm spacings. Dendrites are formed by the crystallization of alloys or impure metals due to microsegregation. Cooling-rate estimates are used in numerical simulations for heat and material transport for a moving heat flux [5–6].

Dendrites are obtained between two limits of growth rate. Below and above this range, microsegregation-free structures can be obtained. Columnar (directional) dendrites are obtained when applying an external, unidirectional, strong, heat flux. The correlations between dendrite spacing and cooling rate have, according to Fleming and co-workers [7–8], the general form

$$\lambda_1 = a\varepsilon^{-n_1}, \quad \lambda_2 = a\varepsilon^{-n_2} \qquad (1)$$

where ε is the cooling rate (K s^{-1}) and λ_1 and λ_2 are the primary- or secondary-dendrite spacings (μm). The constants a, b, n_1 and n_2 are experimentally determined, and they are material dependent. A similar dependence of the dendritic morphology and temperature gradient or growth rate for steel or other alloys was found by Taha [4]. The correlations found at low cooling rates have been extrapolated and applied for high cooling rates [1].

Few experimental data have been published concerning the parametric study of microstructural transformations in rapid solidification.

The aim of the present work is to estimate the cooling rate for high-power-CO_2-laser welding as a function of the beam speed (welding speed) and beam power. The microstructural analysis for 304 L stainless steel obtained for different experimental conditions is compared to recent rapid-solidification models for dendrite growth.

A simple heat-transfer analogy is made between the cooling rate in melt spinning and laser welding. Also, temperature–time measurements were performed in the heat-affected zone, enabling cooling rate estimation very close to the melt pool.

2. Experimental procedures

Welding tests were performed with a continuous-wave CO_2 United Technologies Industrial Lasers (UTIL) laser with a nominal power of 25 kW. The beam-focusing head used in the experiments was adapted with a spherical mirror with an 18.2″ focal length. During the welding tests, the samples were protected by a coaxial shielding gas (helium). The laser beam was stationary and the metal samples were translated at different speeds using a controlled moving table, producing a uniform weld over a distance of 10 cm. The following welding parameters were used: a beam power of 5–17.5 kW and a welding speed of 0.5–10 cm s^{-1}, corresponding to an applied energy of 1–10 kJ cm^{-1}. The focus position was 5 mm below the surface of the welded plates [13].

0022–2461

The material was an austenitic stainless steel (AISI 304 L) either 7 or 14 mm thick. The weld-zone dimensions were analysed after sectioning, polishing and etching with Kalling's reagent. Dendrite-spacing measurements were made at half weld penetration by an intercept method on optical micrographs. The chemical composition of the steel is given in Table I.

Temperature–time measurements [14] were obtained using chromel–alumel thermocouples; each wire was 0.3 mm in diameter. The wires were welded on the surface of the samples, parallel to the weld axis, at a distance of 2 mm. More details can be found in [14]. The response times of the thermocouples were corrected according to Henning and Parker's theory [15].

3. Experimental results

3.1. Dendrite-spacing measurements

The dendrite-spacing data presented in Table II correspond each to mean values of at least 10 separate measurements by the intercept method at half weld penetration. The interdendritic spacings were found to be relatively uniform in the fusion zone (Fig. 1). Some coarser structures were observed close to the top and bottom free surfaces due to slower cooling rates in the inert-gas atmosphere. The slower cooling rates could also be due to increased melt volume in these areas. The dendrite structure revealed by etching is columnar.

Under steady-state welding conditions, the dendrite-growth rate or solidification rate, V, is related to the beam velocity, V_b by the relation: $V = V_b \cos\theta$, where θ is the angle between the normal to the liquid–solid interface and the beam direction. The direction of solidification is along the maximum thermal gradient, that is, normal to the liquid interface. The dendrite-growth rate can, therefore, be replaced by V_b to a good approximation.

The non-dimensional thermal Peclet number, P_t [16] can be calculated from the equation $P_t = rV/(2a)$, where r is the beam radius (0.3 mm), a is the heat-diffusion coefficient (4×10^{-2} cm^2 s^{-1} for 304 L stainless steel) and $V = 0.5$–5 cm s^{-1}. The thermal Peclet number for the experimental conditions investigated was in the range 0.3–1.5. At these low values of

TABLE I Chemical compostion of 304 L steel (wt %)

C	Cr	Ni	S	P	Si	Mn	Fe
0.017	18.18	9.29	0.005	0.025	0.44	1.6	Balance

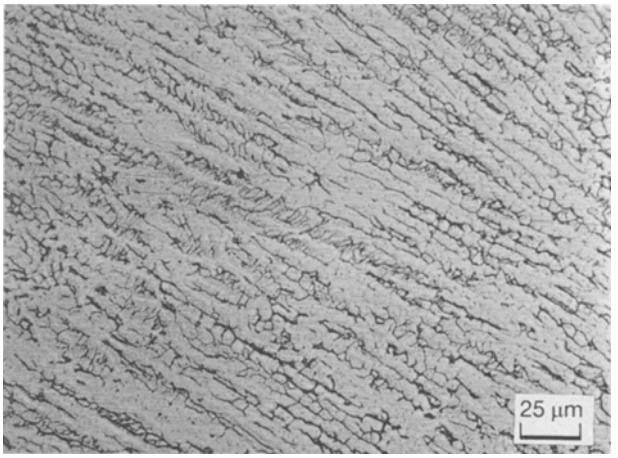

Figure 1 Dendrites in a laser-weld cross-section (×400).

TABLE II Welding experiments, cooling rates and thermal gradients, in 14 mm plate

Experiment	P (kW)	V (cm s^{-1})	E (kJ cm^{-1})	λ_1 (μm)	e (K s^{-1})	G (K cm^{-})
1	5	1.0	5.0	9.9	562	562
2	5	0.75	6.6	9.3	679	905
3	5	0.5	10.0	17.0	109	200
4	5	2.0	2.5	8.0	1072	536
5	7.5	1.5	5.0	13.3	230	153
6	7.5	1.25	6.0	14.9	163	130
7	7.5	1.0	7.5	11.2	386	386
8	7.5	2.0	3.75	10.9	420	210
9	7.5	0.75	10.0	15.8	134	178
10	10	2.0	5.0	6.6	1920	960
11	10	2.5	5.0	8.0	1072	428
12	10	3.0	3.3	7.0	1607	535
13	10	1.5	6.6	9.4	657	438
14	10	4.0	2.5	6.7	1835	458
15	12.5	1.5	8.3	10.0	545	363
16	12.5	2.0	6.2	10.3	498	249
17	12.5	2.5	5.0	6.8	1754	701
18	12.5	3.0	4.1	7.6	1252	417
19	12.5	3.5	3.6	5.8	2841	811
20	12.5	4.0	3.1	6.8	1754	438
21	15	2.0	7.5	11.0	386	193
22	15	3.0	5.0	8.5	892	297
23	17.5	2.0	8.75	13.0	248	124
24	17.5	3.5	5.0	8.3	960	274
25	17.5	4.5	3.9	6.6	1920	426
26	17.5	4.0	4.4	7.0	1607	401
27	17.5	3.0	5.8	7.7	1204	401

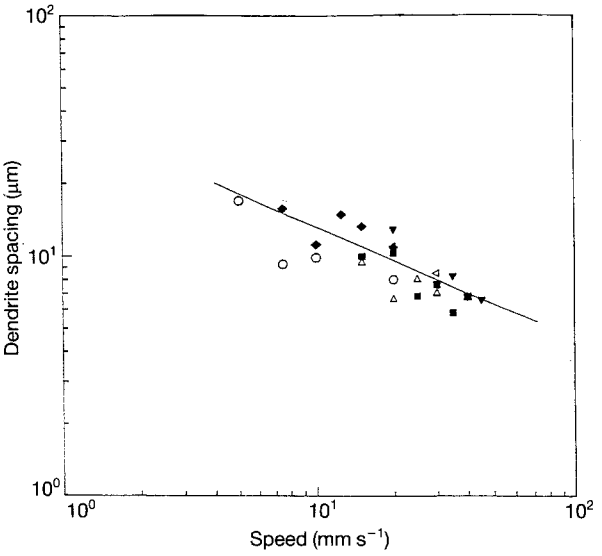

Figure 2 Primary-dendrite spacings as a function of welding speed, at different beam powers for a 14 mm thick stainless-steel plate: (○) 5 kW, (◆) 7.5 kW, (△) 10 kW, (■) 12.5 kW, (◁) 15 kW, and (▼) 17.5 kW.

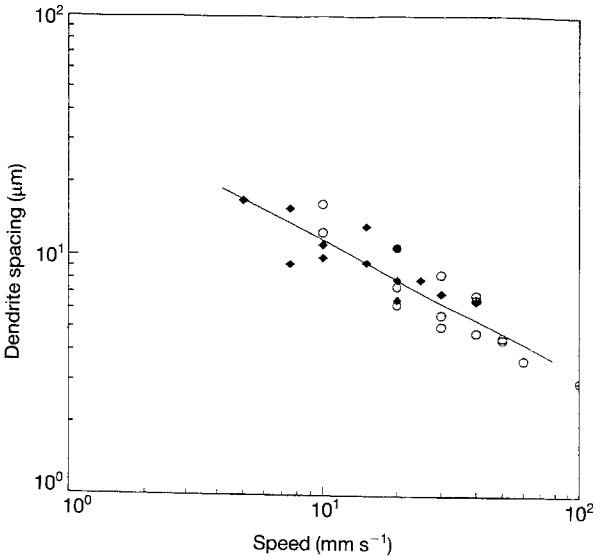

Figure 3 Primary-dendrite spacings as a function of welding speed for different welding parameters for (◆) 7 and (○) 14 mm sample thicknesses.

the thermal Peclet numbers, the velocity of the solidification front is close to that of the beam rate [16].

As can be seen from Fig. 2, a power-law relationship has been found between λ_1 and V for different laser powers. This correlation can be expressed as

$$\lambda_1 = 40V^{-1/2} \quad (2)$$

for λ_1 in μm and V in mm s^{-1}.

Another set of experiments was performed in order to compare changes in microstructure as a function of the sample thickness, the welding speed and the laser power. The results are presented in Table II and Fig. 3. For different experimental parameters, but under steady-state welding conditions, the dendrite spacing depends only on the dendrite-growth rate and it can be given as $\lambda_1 = \text{const } V^{-1/2}$. This conclusion can be confirmed by comparing these experimental results with the recent theoretical models described in Section 4.

3.2. Cooling-rate calculations

Cooling rates, ε, have been inferred from primary-dendrite-spacing measurements using the correlations experimentally determined for stainless steel by Katayama and Matsunawa and also used by Elmer [1]

$$\lambda_1 = 80(\varepsilon)^{-0.33} \quad (3)$$

where λ_1 is in μm and ε is in K s^{-1}.

Temperature gradients were calculated using the relation

$$G = \varepsilon/V \quad (4)$$

where V is the velocity of the solidification front (in cm s^{-1}), and G is the temperature gradient (in K cm^{-1}). The maximum solidification-front velocity, equal to the beam velocity (welding speed), was used in our calculations.

The cooling rates obtained for the experimental parameters were in the range 10^2 to 3×10^3 K s^{-1} and temperature gradients were obtained in the range 1–9 $\times 10^2$ K cm^{-1} (see Table II).

4. Discussion

4.1. Dendrite-growth models

A theoretical model has been developed by Kurz *et al.* [9] and Rappaz and co-workers [10–12] to describe columnar (directional) constrained growth of dendrites including growth rates for the limit of absolute stability. The growth law can be represented by the following equation [10–12]

$$AV^2 + BV + G = 0 \quad (5)$$

where A and B contain material dependent physical and thermodynamic constants. The system is characterized by mass diffusion or a solutal Peclet number, P, defined as $P = RV/2D$, where R is the dendrite-tip radius and D is the diffusion coefficient in the liquid. As a first approximation the dendrite-tip radius [10–12], $R = \lambda_1/2$ (see also Fig. 1). The solution of Equation 5 for our alloy (for a thermal gradient of 500 K cm^{-1}) is presented in Fig. 4. The thermal gradient used in our calculations is the mean value of the experimental thermal gradient (Table II), and it is not an assumed value, as in the model used by Rappaz. The solid curve represents the dendrite growth for a wide range of velocities (0.1–100 cm s^{-1}). Our steady-state welding experiments cover only the part of this range corresponding to the linear region where VR^2 = constant. Dendrites can also be observed at very high velocities of 10 cm s^{-1}, which should be above the limit of absolute stability according to this model.

The absolute limit, corresponding to the smallest dendrite radius, was defined by Kurz and Rappaz as

$$V_{abs} = \Delta T_0 D/\Gamma k \quad (6)$$

where $\Delta T_0 = mc_0(k-1)/k$, m is the liquidus slope in a pseudo-binary system (− 4.3 for our alloy), k is the partition coefficient (0.95), c_0 is the initial Cr concentration (19%) and Γ is the Gibbs–Thompson parameter (1.9×10^{-7} K m) and D is the solutal diffusion coefficient (4.9×10^{-9} m^2 s^{-1} at the liquidus temperature of 1775 K) [9–16]. By substituting the above

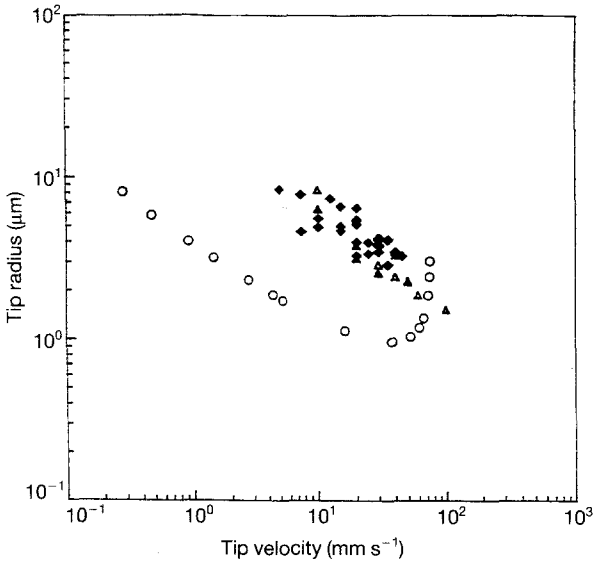

Figure 4 Dendrite-growth results for (○) the model and experimental results for (◆) 7 and (△) 14 mm thick samples.

values for our pseudo-binary system, V_{abs} is about 11 cm s^{-1}. However, it should be remembered that when k and m are estimated by substituting $k = 0.9$ instead of $k = 0.95$ the term $(k - 1)$ will change by a factor of two, and consequently so will the value of the absolute velocity, as can be seen from Equation 6. The same is true with the estimated slope of the liquidus. Therefore, the estimate of the absolute velocity by this approximation is reliable within a factor of two.

The simplified model for dendrite growth proposed by Kurz *et al.* [9] is

$$VR^2 = 4\pi^2 D\Gamma/k\Delta T = \text{constant} \quad (7)$$

This constant calculated for our experimental conditions (with D, Γ, k and ΔT given as above) is 87×10^{-8} cm^3 s^{-1}. Taking $V = 1$ cm s^{-1}, the corresponding tip radius will be $R = 9.3$ μm and $\lambda_1 = 18.6$ μm. This value is in very good agreement with our experimental data.

4.2. An analogy between the cooling rates observed during melt spinning and laser welding

Melt spinning and laser welding are two rapid-solidification methods where heat is rapidly extracted from the melt by contact with a heat sink. In melt spinning, a ribbon of molten material is cooled on a turning metal wheel, while in welding a "ribbon" is formed between two blocks of metal at a speed equal to the welding speed. The thickness of the "welding ribbon" is about 1–2 mm compared with 0.1 mm for melt spun ones. Yet the welds are cooled on both sides.

The cooling rate for melt spinning is usually calculated [17] by the following equation

$$\varepsilon = -h(T - T_W)x\rho C \quad (8)$$

where h is the heat-transfer coefficient, T and T_W are the ribbon and wheel temperature, x, ρ and c are the ribbon thickness, density and specific heat, respectively. By substituting the values $h = 2 \times 10^4$ W cm^{-2} K (an extrapolated value of h for lower speeds from figure 8 in [17]), $x = 2 \times 10^{-3}$ m, $\rho = 7800$ kg m^{-3} and $c = 760$ J kg^{-1} K, and with the temperature difference between the melted metal and the heat-affected zone being about 600 K, we can obtain $\varepsilon = 1040$ K s^{-1}. This estimate of the cooling rate is in agreement with the results obtained by microstructural analysis. Because the heat-transfer coefficient is an extrapolated estimate, the above calculations are reliable within 50%.

4.3. Temperature–time cycles in heat-affected zones

Some thermal measurements were performed in the heat-affected zone using thermocouples welded on the surface of the plate samples. A typical record of temperature as a function of time is given in Fig. 5. The temperature drop with time is not constant, and the steepest slope is at the closest contact with the welding. At this point, the slope $\Delta T/\Delta t =$ 100–300 K s^{-1}. The cooling rate estimated by microstructural analysis for similar experimental conditions

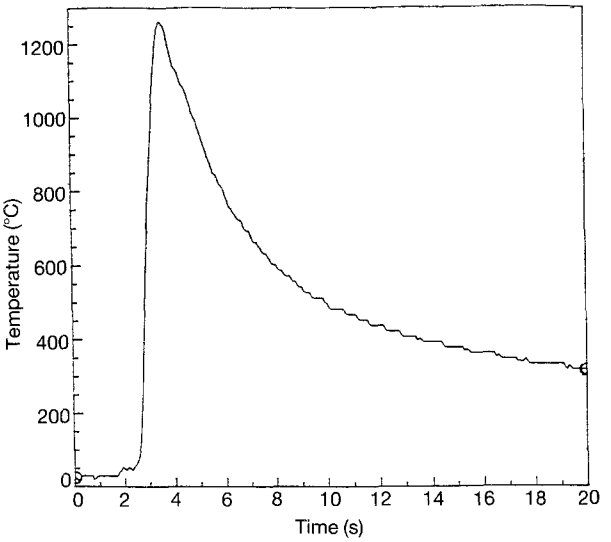

Figure 5 Experimental temperature–time profile in the heat-affected zone during laser welding.

TABLE III Primary-dendrite spacings for different welding parameters, for plate thicknesses of 7 and 14 mm

Power (kW)	7 mm plate		14 mm plate	
	V (cm s^{-1})	λ_1 (μm)	V (cm s^{-1})	λ_1 (μm)
5	1	12.6	0.5	17
	2	6.3	0.75	9.3
	3	5.1	1	9.9
	4	4.8	2	8
7.5	1	16.5	0.75	15.8
	2	10.9	1	11.2
	3	8.4	1.5	13.3
	4	6.9	2	10.9
	5	4.5		
10	2	7.5	1.5	9.5
	3	5.7	2	6.6
	4	6.6	2.5	8
	5	4.6	3	7
	6	3.7	3	7
	10	3	4	6.5

(7 kW, 1.2 cm s^{-1}) resulted in cooling rates of 163 K s^{-1} (see Table II). This method is also an estimate of the cooling rate, but its accuracy is very much dependent on the thermocouple mounting and response time.

5. Conclusion

A high-power laser was used to perform a parametric study of microstructural transformations during laser welding in order to estimate cooling rates and temperature gradients in 304 L stainless-steel welds. The experimental results can be represented as a power-law dependence between the primary-dendrite spacing and the welding speed for different laser powers. The experimental correlation $\lambda_1 = 40V^{-1/2}$ (for spacings in μm and speeds in mm s^{-1}) is in very good agreement with recent models of dendrite growth. The cooling rates estimated by the dendrite-spacing correlations were found to be in the range 10^2 to 3×10^3 K s^{-1}, for the experimental parameters investigated. Temperature variation with time in the heat-affected zone measured with a thermocouple also gives analogous indications of the cooling rate. An analogy concerning the cooling rate was shown to exist between laser welding and melt spinning. The cooling rate estimated by this analogy is about 10^3 K s^{-1}, while the temperature-drop measurement in the heat-affected zone resulted in a value of about 1.5×10^2 K s^{-1}.

References

1. J. W. ELMER, S. M. ALLEN and T. W. EAGER, *Metall. Trans. A* **20** (1989) 2117–2131.
2. P. A. MOLIAN, *J. Mater. Sci. Lett.* **4** (1985) 265–267.
3. S. KATAYAMA and A. MATSUNAWA, Proceedings of ICALEO (1984) pp. 60–67.
4. M. A. TAHA, *J. Mater. Sci. Lett.* **5** (1986) 307–310.
5. M. RAPPAZ, B. CARRUPT, M. ZIMMERMAN and W. KURZ, *Helvetica, Phys. Acta* **60** (1987) 924–936.
6. C. L. CHAN, J. MAZUMER and M. M. CHEN, *J. Appl. Phys.* **64** (1988) 6166–6174.
7. W. E. BROWER, R. STRACHAN and M. C. FLEMING, *AFS Cast. Met. Res.* **12** (1970) 176.
8. M. C. FLEMING, "Solidification processing" (McGraw Hill, New York, 1974) pp. 146 ff.
9. W. KURZ, B. GIOVANOLA and R. TRIVEDI, *Acta Metall.* **34** (1986) 823–830.
10. M. RAPPAZ, S. A. DAVID, J. M. VITEK and L. BOATNER, *Metall. Trans. A* **20** (1989) 1125–1138.
11. S. A. DAVID, J. M. VITEK, M. RAPPAZ and L. A. BOATNER, *ibid.* **21** (1990) 1767–1782.
12. M. RAPPAZ, S. A. DAVID, J. M. VITEK and L. A. BOATNER, *ibid.* **21** (1990) 1767–1782.
13. B. DABEZIES, E. RANCHY and J. M. SIGNAMARCHEIX, Proceedings of ICALEO, October (1989) Orlando.
14. B. DABEZIES, L. GAUTHIER and J. M. SIGNAMARCHEIX, OPTO, September to October (1990) Paris, pp. 16–23.
15. C. H. HENNING and R. PARKER, *Trans. ASME*, May (1967) 146–154.
16. M. RAPPAZ, M. GREMAUD, R. DEKUMBIS and W. KURZ, European Conference of Laser Treatment of Materials, edited by B. L. Mortike (Information-gesellschaft Verlag, Bad Neuheim, 1986) pp. 43–53.
17. B. P. BEWLAY and B. CANTOR, *Int. J. Rapid Solidification* **2** (1986) 107–123.

Received 13 October 1992
and accepted 6 October 1993